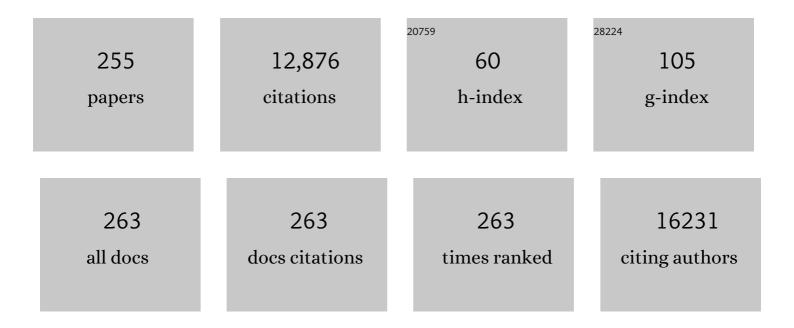
List of Publications by Year in descending order

Source: https://exaly.com/author-pdf/9132550/publications.pdf Version: 2024-02-01



#	Article	IF	CITATIONS
1	Optical properties of the ZnO nanotubes synthesized via vapor phase growth. Applied Physics Letters, 2003, 83, 1689-1691.	1.5	616
2	A Highâ€Rate and Stable Quasiâ€Solidâ€State Zincâ€lon Battery with Novel 2D Layered Zinc Orthovanadate Array. Advanced Materials, 2018, 30, e1803181.	11.1	571
3	Efficient field emission from ZnO nanoneedle arrays. Applied Physics Letters, 2003, 83, 144-146.	1.5	497
4	A Scalable General Synthetic Approach toward Ultrathin Imine-Linked Two-Dimensional Covalent Organic Framework Nanosheets for Photocatalytic CO ₂ Reduction. Journal of the American Chemical Society, 2019, 141, 17431-17440.	6.6	418
5	Fiberâ€Based Flexible Allâ€Solidâ€State Asymmetric Supercapacitors for Integrated Photodetecting System. Angewandte Chemie - International Edition, 2014, 53, 1849-1853.	7.2	387
6	Ternary oxide nanostructured materials for supercapacitors: a review. Journal of Materials Chemistry A, 2015, 3, 10158-10173.	5.2	320
7	Atomic layer deposited TiO ₂ on a nitrogen-doped graphene/sulfur electrode for high performance lithium–sulfur batteries. Energy and Environmental Science, 2016, 9, 1495-1503.	15.6	320
8	Shape-Controlled Synthesis of Co ₂ P Nanostructures and Their Application in Supercapacitors. ACS Applied Materials & amp; Interfaces, 2016, 8, 3892-3900.	4.0	319
9	Flexible coaxial-type fiber supercapacitor based on NiCo2O4 nanosheets electrodes. Nano Energy, 2014, 8, 44-51.	8.2	248
10	Synthesis of large arrays of aligned α-Fe2O3 nanowires. Chemical Physics Letters, 2003, 379, 373-379.	1.2	242
11	Synthesis, optical, and magnetic properties of diluted magnetic semiconductor Zn1â^xMnxO nanowires via vapor phase growth. Applied Physics Letters, 2003, 83, 4020-4022.	1.5	214
12	Low-temperature growth and Raman scattering study of vertically aligned ZnO nanowires on Si substrate. Applied Physics Letters, 2003, 83, 4631-4633.	1.5	194
13	Tip-Enhanced Raman Spectroscopy. Analytical Chemistry, 2016, 88, 9328-9346.	3.2	180
14	Plasmon-exciton coupling of monolayer MoS2-Ag nanoparticles hybrids for surface catalytic reaction. Materials Today Energy, 2017, 5, 72-78.	2.5	169
15	Facile Growth of Caterpillar-like NiCo ₂ S ₄ Nanocrystal Arrays on Nickle Foam for High-Performance Supercapacitors. ACS Applied Materials & Interfaces, 2017, 9, 18774-18781.	4.0	165
16	Low-temperature growth and properties of ZnO nanowires. Applied Physics Letters, 2004, 84, 4941-4943.	1.5	163
17	Freestanding and Sandwichâ€Structured Electrode Material with High Areal Mass Loading for Longâ€Life Lithium–Sulfur Batteries. Advanced Energy Materials, 2017, 7, 1602347.	10.2	159
18	Bimetallic nanostructures with magnetic and noble metals and their physicochemical applications. Progress in Natural Science: Materials International, 2013, 23, 113-126.	1.8	143

#	Article	IF	CITATIONS
19	Green-light-emitting ZnSe nanowires fabricated via vapor phase growth. Applied Physics Letters, 2003, 82, 3330-3332.	1.5	140
20	Ribbon- and Boardlike Nanostructures of Nickel Hydroxide:Â Synthesis, Characterization, and Electrochemical Properties. Journal of Physical Chemistry B, 2005, 109, 7654-7658.	1.2	139
21	An investigation on the microstructure of an AM50 magnesium alloy. Materials Science & Engineering A: Structural Materials: Properties, Microstructure and Processing, 2003, 355, 201-207.	2.6	131
22	Surfactant-Directed Polypyrrole/CNT Nanocables: Synthesis, Characterization, and Enhanced Electrical Properties. ChemPhysChem, 2004, 5, 998-1002.	1.0	130
23	Interconnected hierarchical NiCo ₂ O ₄ microspheres as high-performance electrode materials for supercapacitors. Dalton Transactions, 2017, 46, 9201-9209.	1.6	128
24	Cationic surfactant directed polyaniline/CNT nanocables: synthesis, characterization, and enhanced electrical properties. Carbon, 2004, 42, 1455-1461.	5.4	126
25	Vibrational spectroscopy of phthalocyanine and naphthalocyanine in sandwich-type (na)phthalocyaninato and porphyrinato rare earth complexes. Vibrational Spectroscopy, 2006, 40, 47-54.	1.2	126
26	Bicrystalline Hematite Nanowires. Journal of Physical Chemistry B, 2005, 109, 12245-12249.	1.2	123
27	Facile synthesis of AgBr nanoplates with exposed {111} facets and enhanced photocatalytic properties. Chemical Communications, 2012, 48, 275-277.	2.2	123
28	Porous nanotubes of Co3O4: Synthesis, characterization, and magnetic properties. Applied Physics Letters, 2004, 85, 2080-2082.	1.5	122
29	Interfacial electronic structure modulation of Pt-MoS2 heterostructure for enhancing electrocatalytic hydrogen evolution reaction. Nano Energy, 2022, 94, 106913.	8.2	119
30	An efficient ruthenium catalyst for selective hydrogenation of ortho-chloronitrobenzene prepared via assembling ruthenium and tin oxide nanoparticles. Journal of Catalysis, 2004, 222, 493-498.	3.1	113
31	Orientation-Controlled Growth of Single-Crystal Silicon-Nanowire Arrays. Advanced Materials, 2005, 17, 56-61.	11.1	112
32	Uniform Metal Nanotube Arrays by Multistep Template Replication and Electrodeposition. Advanced Materials, 2004, 16, 1550-1553.	11.1	107
33	Magnetic nanochains of metal formed by assembly of small nanoparticles. Chemical Communications, 2004, , 2726.	2.2	106
34	Synthesis, Microstructure, and Growth Mechanism of Dendrite ZnO Nanowires. Journal of Physical Chemistry B, 2003, 107, 8289-8293.	1.2	101
35	Amplifying fluorescence sensing based on inverse opal photonic crystal toward trace TNT detection. Journal of Materials Chemistry, 2011, 21, 1730-1735.	6.7	101
36	Facile Synthesis of Monodisperse Mn3O4 Tetragonal Nanoparticles and Their Large-Scale Assembly into Highly Regular Walls by a Simple Solution Route. Small, 2007, 3, 606-610.	5.2	99

#	Article	IF	CITATIONS
37	Ni/Ni ₃ C Core–Shell Nanochains and Its Magnetic Properties: One-Step Synthesis at Low Temperature. Nano Letters, 2008, 8, 1147-1152.	4.5	99
38	Substrate induced changes in atomically thin 2-dimensional semiconductors: Fundamentals, engineering, and applications. Applied Physics Reviews, 2017, 4, 011301.	5.5	97
39	Growth and formation mechanism of c-oriented ZnO nanorod arrays deposited on glass. Journal of Crystal Growth, 2004, 269, 464-471.	0.7	96
40	High-Quality Ultra-Fine GaN Nanowires Synthesized Via Chemical Vapor Deposition. Advanced Materials, 2003, 15, 419-421.	11.1	93
41	Core@shell CoO@Co 3 O 4 nanocrystals assembling mesoporous microspheres for high performance asymmetric supercapacitors. Chemical Engineering Journal, 2017, 327, 100-108.	6.6	93
42	Amplification of Fluorescent Contrast by Photonic Crystals in Optical Storage. Advanced Materials, 2010, 22, 1237-1241.	11.1	91
43	Hollow Co ₂ P nanoflowers assembled from nanorods for ultralong cycle-life supercapacitors. Nanoscale, 2017, 9, 14162-14171.	2.8	89
44	Synthesis of Nickel Hydroxide Nanoribbons with a New Phase:Â A Solution Chemistry Approach. Journal of Physical Chemistry B, 2004, 108, 7531-7533.	1.2	85
45	Attachment-Driven Morphology Evolvement of Rectangular ZnO Nanowires. Journal of Physical Chemistry B, 2005, 109, 8786-8790.	1.2	85
46	Platinum catalyzed growth of NiPt hollow spheres with an ultrathin shell. Journal of Materials Chemistry, 2011, 21, 1925-1930.	6.7	84
47	Complementary Charge Trapping and Ionic Migration in Resistive Switching of Rare-Earth Manganite TbMnO ₃ . ACS Applied Materials & Interfaces, 2013, 5, 1213-1217.	4.0	84
48	Fabrication and microstructure analysis on zinc oxide nanotubes. New Journal of Physics, 2003, 5, 115-115.	1.2	83
49	Nanotubular structures of zinc oxide. Solid State Communications, 2004, 129, 671-675.	0.9	83
50	Stability investigation of a high number density Pt ₁ /Fe ₂ O ₃ single-atom catalyst under different gas environments by HAADF-STEM. Nanotechnology, 2018, 29, 204002.	1.3	83
51	Microsized BiOCl Square Nanosheets as Ultraviolet Photodetectors and Photocatalysts. ACS Applied Materials & Interfaces, 2016, 8, 6662-6668.	4.0	81
52	Optical, photonic and optoelectronic properties of graphene, h-BN and their hybrid materials. Nanophotonics, 2017, 6, 943-976.	2.9	78
53	Extraordinary electrocatalytic performance for formic acid oxidation by the synergistic effect of Pt and Au on carbon black. Nano Energy, 2018, 48, 1-9.	8.2	77
54	Au/Ni12P5 core/shell nanocrystals from bimetallic heterostructures: in situ synthesis, evolution and supercapacitor properties. NPG Asia Materials, 2014, 6, e122-e122.	3.8	76

#	Article	IF	CITATIONS
55	FePt Icosahedra with Magnetic Cores and Catalytic Shells. Journal of Physical Chemistry C, 2009, 113, 4395-4400.	1.5	74
56	Enhanced Catalytic Activities of NiPt Truncated Octahedral Nanoparticles toward Ethylene Glycol Oxidation and Oxygen Reduction in Alkaline Electrolyte. ACS Applied Materials & Interfaces, 2016, 8, 10841-10849.	4.0	74
57	Microstructures and dislocations in the stressed AZ91D magnesium alloys. Materials Science & Engineering A: Structural Materials: Properties, Microstructure and Processing, 2003, 344, 279-287.	2.6	72
58	Large-Scale Synthesis of Uniform Nanotubes of a Nickel Complex by a Solution Chemical Route. Journal of the American Chemical Society, 2004, 126, 4530-4531.	6.6	68
59	Phase formations and magnetic properties of single crystal nickel ferrite (NiFe ₂ O ₄) with different morphologies. CrystEngComm, 2015, 17, 1603-1608.	1.3	67
60	Shape controllable synthesis of ZnO nanorod arrays via vapor phase growth. Solid State Communications, 2004, 129, 803-807.	0.9	58
61	Highly efficient hydrogen production and formaldehyde degradation by Cu2O microcrystals. Applied Catalysis B: Environmental, 2015, 172-173, 1-6.	10.8	58
62	Ni(OH)2@Co(OH)2 hollow nanohexagons: Controllable synthesis, facet-selected competitive growth and capacitance property. Nano Energy, 2014, 5, 52-59.	8.2	56
63	Monodispersed, ultrathin NiPt hollow nanospheres with tunable diameter and composition via a green chemical synthesis. Journal of Materials Chemistry A, 2015, 3, 1031-1036.	5.2	55
64	TEM investigation on the growth mechanism of carbon nanotubes synthesized by hot-filament chemical vapor deposition. Micron, 2004, 35, 455-460.	1.1	53
65	Effect of adsorbates on field-electron emission from ZnO nanoneedle arrays. Journal of Applied Physics, 2004, 96, 624-628.	1.1	50
66	Fluorescence enhancement by heterostructure colloidal photonic crystals with dual stopbands. Journal of Colloid and Interface Science, 2011, 356, 63-68.	5.0	50
67	Tailoring surface phase transition and magnetic behaviors in BiFeO3 via doping engineering. Scientific Reports, 2015, 5, 9128.	1.6	50
68	Atomic-scaled surface engineering Ni-Pt nanoalloys towards enhanced catalytic efficiency for methanol oxidation reaction. Nano Research, 2020, 13, 3088-3097.	5.8	50
69	One-Pot Synthesis of Highly Crystallined λ-MnO ₂ Nanodisks Assembled from Nanoparticles: Morphology Evolutions and Phase Transitions. Journal of Physical Chemistry C, 2008, 112, 365-369.	1.5	49
70	Au/Ni12P5 core/shell single-crystal nanoparticles as oxygen evolution reaction catalyst. Nano Research, 2017, 10, 3103-3112.	5.8	48
71	Synergy between β-Mo2C Nanorods and Non-thermal Plasma for Selective CO2 Reduction to CO. CheM, 2020, 6, 3312-3328.	5.8	47
72	Synthesis and Electrochemical Properties of Porous α-Co(OH) 2 and Co 3 O 4 Microspheres. Progress in Natural Science: Materials International, 2017, 27, 197-202.	1.8	47

#	Article	IF	CITATIONS
73	Structural stability of icosahedral FePt nanoparticles. Nanoscale, 2009, 1, 276.	2.8	46
74	Tuning oxygen vacancy photoluminescence in monoclinic Y2WO6 by selectively occupying yttrium sites using lanthanum. Scientific Reports, 2015, 5, 9443.	1.6	46
75	Layer-controlled Pt-Ni porous nanobowls with enhanced electrocatalytic performance. Nano Research, 2017, 10, 187-198.	5.8	46
76	Oriented-assembly of hollow FePt nanochains with tunable catalytic and magnetic properties. Nanoscale, 2016, 8, 11432-11440.	2.8	45
77	Atom-Resolved Evidence of Anisotropic Growth in ZnS Nanotetrapods. Nano Letters, 2011, 11, 2983-2988.	4.5	43
78	Well-Aligned CoPt Hollow Nanochains Synthesized in Water at Room Temperature. Journal of Physical Chemistry C, 2012, 116, 5352-5357.	1.5	41
79	Nanostructure Optimization of Platinum-Based Nanomaterials for Catalytic Applications. Nanomaterials, 2018, 8, 949.	1.9	40
80	Microfluidic Synthesis and Characterization of FePtSn/C Catalysts with Enhanced Electro-Catalytic Performance for Direct Methanol Fuel Cells. Electrochimica Acta, 2017, 230, 245-254.	2.6	39
81	Atomic Scale Stability of Tungsten–Cobalt Intermetallic Nanocrystals in Reactive Environment at High Temperature. Journal of the American Chemical Society, 2019, 141, 5871-5879.	6.6	39
82	Magnetic and transport and dielectric properties of polycrystalline TbMnO3. Solid State Communications, 2006, 138, 481-484.	0.9	37
83	Promoting methanol-oxidation-reaction by loading PtNi nano-catalysts on natural graphitic-nano-carbon. Electrochimica Acta, 2020, 353, 136542.	2.6	37
84	Thermal evaporation synthesis of zinc oxide nanowires. Applied Physics A: Materials Science and Processing, 2005, 80, 1527-1530.	1.1	36
85	Ferroelectricity-induced performance enhancement of V-doped ZnO/Si photodetector by direct energy band modulation. Nano Energy, 2019, 65, 104046.	8.2	36
86	Structure design, controllable synthesis, and application of metal-semiconductor heterostructure nanoparticles. Progress in Natural Science: Materials International, 2020, 30, 1-12.	1.8	36
87	Atomic origins of the strong metal–support interaction in silica supported catalysts. Chemical Science, 2021, 12, 12651-12660.	3.7	36
88	Carbon-Involved Near-Surface Evolution of Cobalt Nanocatalysts: An in Situ Study. CCS Chemistry, 2021, 3, 154-167.	4.6	36
89	Photoresponsive Covalent Organic Frameworks with Diarylethene Switch for Tunable Singlet Oxygen Generation. Chemistry of Materials, 2022, 34, 1956-1964.	3.2	35
90	Morphology–structure diversity of ZnS nanostructures and their optical properties. Rare Metals, 2014, 33, 1-15.	3.6	33

#	Article	IF	CITATIONS
91	Controlled fabrication, lasing behavior and excitonic recombination dynamics in single crystal CH3NH3PbBr3 perovskite cuboids. Science Bulletin, 2019, 64, 698-704.	4.3	33
92	Nanomagnetic CoPt truncated octahedrons: facile synthesis, superior electrocatalytic activity and stability for methanol oxidation. Science China Materials, 2017, 60, 57-67.	3.5	32
93	Controlled synthesis of monodispersed hematite microcubes and their properties. CrystEngComm, 2011, 13, 7114.	1.3	31
94	<i>In Situ</i> Redox Microfluidic Synthesis of Core–Shell Nanoparticles and Their Long-Term Stability. Journal of Physical Chemistry C, 2013, 117, 17274-17284.	1.5	31
95	A General Strategy for Nanohybrids Synthesis via Coupled Competitive Reactions Controlled in a Hybrid Process. Scientific Reports, 2015, 5, 9189.	1.6	31
96	Surface and interface engineering of FePt/C nanocatalysts for electro-catalytic methanol oxidation: enhanced activity and durability. Nanoscale, 2017, 9, 4066-4075.	2.8	31
97	Microstructure and interface structure studies of SiCp-reinforced Al (6061) metal-matrix composites. Materials Science & Engineering A: Structural Materials: Properties, Microstructure and Processing, 1998, 254, 219-226.	2.6	30
98	Effect of rare earth on the microstructures and properties of a low expansion superalloy. Journal of Alloys and Compounds, 2000, 311, 60-64.	2.8	29
99	Defects and growing mechanisms of α-Fe2O3 nanowires. Chemical Physics Letters, 2006, 431, 100-103.	1.2	29
100	From ZnS nanoparticles, nanobelts, to nanotetrapods: the ethylenediamine modulated anisotropic growth of ZnS nanostructures. Nanoscale, 2012, 4, 2394.	2.8	29
101	TEM investigations on ZnO nanobelts synthesized via a vapor phase growth. Micron, 2004, 35, 481-487.	1.1	28
102	From ZnS nanobelts to ZnO/ZnS heterostructures: Microscopy analysis and their tunable optical property. Applied Physics Letters, 2010, 97, 041916.	1.5	28
103	Magneto-Plasmons in Periodic Nanoporous Structures. Scientific Reports, 2014, 4, .	1.6	28
104	Probing Evolution of Local Strain at MoS ₂ -Metal Boundaries by Surface-Enhanced Raman Scattering. ACS Applied Materials & Interfaces, 2018, 10, 40246-40254.	4.0	28
105	Magnetite hollow spheres: solution synthesis, phase formation and magnetic property. Journal of Nanoparticle Research, 2011, 13, 213-220.	0.8	27
106	Controlled hybridization of Sn–SnO ₂ nanoparticles via simple-programmed microfluidic processes for tunable ultraviolet and blue emissions. Journal of Materials Chemistry C, 2014, 2, 7687-7694.	2.7	27
107	NiPt hollow nanocatalyst: Green synthesis, size control and electrocatalysis. Progress in Natural Science: Materials International, 2014, 24, 175-178.	1.8	27
108	Highly Efficient Metal-Free Two-Dimensional Luminescent Melem Nanosheets for Bioimaging. ACS Applied Materials & Interfaces, 2020, 12, 2145-2151.	4.0	27

#	Article	IF	CITATIONS
109	Phase formation, magnetic and optical properties of epitaxially grown icosahedral Au@Ni nanoparticles with ultrathin shells. CrystEngComm, 2013, 15, 2527.	1.3	26
110	Direct observation of epitaxial alignment of Au on MoS2 at atomic resolution. Nano Research, 2019, 12, 947-954.	5.8	26
111	Anisotropy of two-dimensional ReS2 and advances in its device application. Rare Metals, 2021, 40, 3357-3374.	3.6	26
112	Precise synthesis of Fe–N2 with N vacancies coordination for boosting electrochemical artificial N2 fixation. Applied Catalysis B: Environmental, 2021, 293, 120216.	10.8	26
113	Controllable synthesis of Ni(OH) ₂ /Co(OH) ₂ hollow nanohexagons wrapped in reduced graphene oxide for supercapacitors. RSC Advances, 2016, 6, 97172-97179.	1.7	25
114	Enhanced photoresponse of TiO2/MoS2 heterostructure phototransistors by the coupling of interface charge transfer and photogating. Nano Research, 2021, 14, 982-991.	5.8	25
115	Single-mode lasing of CsPbBr ₃ perovskite NWs enabled by the Vernier effect. Nanoscale, 2021, 13, 4432-4438.	2.8	25
116	In situ tracing of atom migration in Pt/NiPt hollow spheres during catalysis of CO oxidation. Chemical Communications, 2014, 50, 1804.	2.2	24
117	Epitaxy of 2D Materials toward Single Crystals. Advanced Science, 2022, 9, e2105201.	5.6	24
118	Visible light initiated and collapsed resistive switching in TbMnO3/Nb:SrTiO3 heterojunctions. Physical Chemistry Chemical Physics, 2013, 15, 6804.	1.3	23
119	Interface-dependent rectifying TbMnO3-based heterojunctions. AIP Advances, 2011, 1, .	0.6	22
120	From channeled to hollow CoO octahedra: controlled growth, structural evolution and energetic applications. CrystEngComm, 2016, 18, 6849-6859.	1.3	22
121	The dynamics of the peel. Nature Catalysis, 2020, 3, 333-334.	16.1	22
122	Modulating reaction pathways of formic acid oxidation for optimized electrocatalytic performance of PtAu/CoNC. Nano Research, 2022, 15, 1221-1229.	5.8	22
123	Single-molecule field effect and conductance switching driven by electric field and proton transfer. Science Advances, 2022, 8, eabm3541.	4.7	22
124	Antiferromagnetic element Mn modified PtCo truncated octahedral nanoparticles with enhanced activity and durability for direct methanol fuel cells. Nano Research, 2019, 12, 2520-2527.	5.8	21
125	Ultrathin Ni12P5 nanoplates for supercapacitor applications. Journal of Alloys and Compounds, 2019, 782, 545-555.	2.8	21
126	Nanostructured stars of ZnO microcrystals with intense stimulated emission. Applied Physics Letters, 2005, 87, 163103.	1.5	20

#	Article	IF	CITATIONS
127	Flower-Like Nickel Nanocrystals: Facile Synthesis, Shape Evolution, and Their Magnetic Properties. European Journal of Inorganic Chemistry, 2010, 2010, 2261-2265.	1.0	20
128	Interface control and catalytic performances of Au-NiS heterostructures. Chemical Engineering Journal, 2020, 382, 122794.	6.6	20
129	Morphology/phase-dependent MoS2 nanostructures for high-efficiency electrochemical activity. Journal of Alloys and Compounds, 2020, 818, 152909.	2.8	20
130	Dielectric properties of polycrystalline MgB2. Physica C: Superconductivity and Its Applications, 2006, 442, 29-32.	0.6	19
131	Backward rectifying and forward Schottky behavior at Auâ^•Nb-1.0wt%-doped SrTiO3 interface. Applied Physics Letters, 2007, 91, 233513.	1.5	19
132	In situ atom-resolved tracing of element diffusion in NiAu nanospindles. Nanoscale, 2013, 5, 5067.	2.8	19
133	Non-symmetric hybrids of noble metal-semiconductor: Interplay of nanoparticles and nanostructures in formation dynamics and plasmonic applications. Progress in Natural Science: Materials International, 2017, 27, 157-168.	1.8	19
134	Fe doped NiS nanosheet arrays grown on carbon fiber paper for a highly efficient electrocatalytic oxygen evolution reaction. Nanoscale Advances, 2022, 4, 1220-1226.	2.2	19
135	Magnetic anisotropy and anomalous transitions in TbMnO ₃ thin films. Applied Physics Letters, 2012, 101, 122406.	1.5	18
136	Large-scale synthesis of gold dendritic nanostructures for surface enhanced Raman scattering. CrystEngComm, 2015, 17, 4200-4204.	1.3	18
137	Pd–Zn nanocrystals for highly efficient formic acid oxidation. Catalysis Science and Technology, 2018, 8, 4757-4765.	2.1	18
138	Enhanced OER Performances of Au@NiCo2S4 Core-Shell Heterostructure. Nanomaterials, 2020, 10, 611.	1.9	18
139	Microstructure-dependent dielectric properties of TbMnO3 in Auâ^•TbMnO3â^•YBa2Cu3O7â^'x capacitors. Journal of Applied Physics, 2006, 100, 034101.	1.1	17
140	Fast synthesis of uniform mesoporous titania submicrospheres with high tap densities for high-volumetric performance Li-ion batteries. Science China Materials, 2017, 60, 304-314.	3.5	17
141	Structure and Basic Properties of Ternary Metal Oxides and Their Prospects for Application in Supercapacitors. , 2017, , 99-132.		17
142	Direct observation of the hysteretic Fermi level modulation in monolayer MoS2 field effect transistors. Current Applied Physics, 2020, 20, 298-303.	1.1	17
143	Thermodynamic Phase Formation of Morphology and Size Controlled Ni Nanochains by Temperature and Magnetic Field. Journal of Physical Chemistry C, 2010, 114, 7721-7726.	1.5	16
144	A novel non-enzymatic hydrogen peroxide sensor based on Co:ZnO modified electrodes. Progress in Natural Science: Materials International, 2018, 28, 24-27.	1.8	16

#	Article	IF	CITATIONS
145	Solution phase synthesis of magnesium hydroxide sulfate hydrate nanoribbons. Nanotechnology, 2004, 15, 1625-1627.	1.3	15
146	Boron carbide nanowires with uniform CNxcoatings. New Journal of Physics, 2007, 9, 13-13.	1.2	15
147	Thickness-dependent rectifying behavior in heterojunctions of TbMnO3/Nb-1.0Âwt.%-doped SrTiO3. Thin Solid Films, 2008, 516, 2292-2295.	0.8	15
148	Controlled synthesis of Ni0.25Co0.75(OH)2nanoplates and their electrochemical properties. CrystEngComm, 2015, 17, 4859-4864.	1.3	15
149	Low Pt Alloyed Nanostructures for Fuel Cells Catalysts. Catalysts, 2018, 8, 538.	1.6	15
150	Raman spectra study of p -tert-butylphenoxy-substituted phthalocyanines with different central metal and substitution positions. Vibrational Spectroscopy, 2018, 96, 26-31.	1.2	14
151	Magnetic field modulated SERS enhancement of CoPt hollow nanoparticles with sizes below 10 nm. Nanoscale, 2018, 10, 12650-12656.	2.8	14
152	Catalysis of hydrogen evolution reaction by Ni ₁₂ P ₅ single crystalline nanoplates and spherical nanoparticles. CrystEngComm, 2019, 21, 228-235.	1.3	14
153	High Efficiency and Narrow Emission Band Pure-Red Perovskite Colloidal Quantum Wells. Journal of Physical Chemistry Letters, 2021, 12, 10735-10741.	2.1	14
154	Analytical TEM investigations on boron carbonitride nanotubes grown via chemical vapour deposition. New Journal of Physics, 2004, 6, 78-78.	1.2	13
155	Double-layered NiPt nanobowls with ultrathin shell synthesized in water at room temperature. CrystEngComm, 2012, 14, 5151.	1.3	13
156	Functional chemically modified graphene film: microstructure and electrical transport behavior. Journal Physics D: Applied Physics, 2017, 50, 435101.	1.3	13
157	Morphology-Controlled Synthesis of Hematite Nanocrystals and Their Optical, Magnetic and Electrochemical Performance. Nanomaterials, 2018, 8, 41.	1.9	13
158	Atomic Scale Evolution of Graphitic Shells Growth via Pyrolysis of Cobalt Phthalocyanine. Advanced Materials Interfaces, 2020, 7, 2001112.	1.9	13
159	In-situ transmission electron microscopy for probing the dynamic processes in materials. Journal Physics D: Applied Physics, 2021, 54, 443002.	1.3	13
160	Atomâ€Resolved Investigation on Dynamic Nucleation and Growth of Platinum Nanocrystals. Small Methods, 2022, 6, e2200171.	4.6	13
161	Magnetism in undoped ZnS nanotetrapods. Physical Chemistry Chemical Physics, 2013, 15, 2405.	1.3	12
162	Magnetic properties of α-Fe2O3 nanopallets. Rare Metals, 2019, 38, 14-19.	3.6	12

#	Article	IF	CITATIONS
163	Evolution of local strain in Ag-deposited monolayer MoS ₂ modulated by interface interactions. Nanoscale, 2019, 11, 22432-22439.	2.8	12
164	Vibrational spectroscopy of phthalocyanine and naphthalocyanine in sandwich-type (na)phthalocyaninato and porphyrinato rare earth complexes. Polyhedron, 2006, 25, 1195-1203.	1.0	11
165	Single-crystal MgB2 hexagonal microprisms via hybrid physical-chemical vapor deposition. CrystEngComm, 2011, 13, 3959.	1.3	11
166	Tuning giant anomalous Hall resistance ratio in perpendicular Hall balance. Applied Physics Letters, 2015, 106, 152401.	1.5	11
167	Porous Pt–NiO _x nanostructures with ultrasmall building blocks and enhanced electrocatalytic activity for the ethanol oxidation reaction. RSC Advances, 2018, 8, 698-705.	1.7	11
168	Wavelength tunable single-mode lasing from cesium lead halide perovskite microwires. Applied Physics Letters, 2021, 118, .	1.5	11
169	Co2P nanostructures by thermal decomposition: phase formation and magnetic properties. CrystEngComm, 2012, 14, 1197-1200.	1.3	10
170	Preparation and properties of tungsten-doped indium oxide thin films. Rare Metals, 2012, 31, 158-163.	3.6	10
171	Phase formations, magnetic and catalytic properties of Co3O4 hexagonal micro-boxes with one-dimensional nanotubes. CrystEngComm, 2013, 15, 3587.	1.3	10
172	Giant enhancement and anomalous temperature dependence of magnetism in monodispersed NiPt2 nanoparticles. Nano Research, 2017, 10, 3238-3247.	5.8	10
173	Controlled growth of Au/Ni bimetallic nanocrystals with different nanostructures. Rare Metals, 2017, 36, 229-235.	3.6	10
174	Planar Fully Stretchable Lithium-Ion Batteries Based on a Lamellar Conductive Elastomer. ACS Applied Materials & Interfaces, 2020, 12, 53774-53780.	4.0	10
175	In-situ etching synthesis of 3D self-supported serrated Ni-WO3 for oxygen evolution reaction. Journal of Alloys and Compounds, 2022, 893, 162134.	2.8	10
176	A subtle functional design of hollow CoP@MoS2 hetero-nanoframes with excellent hydrogen evolution performance. Materials and Design, 2021, 211, 110165.	3.3	10
177	Improvement of fabrication precision of focused ion beam by introducing simultaneous electron beam. Progress in Natural Science: Materials International, 2010, 20, 111-115.	1.8	9
178	Electrical characteristics of Au and Ag Schottky contacts on Nb-1.0 wt %-doped SrTiO3. Journal of Applied Physics, 2010, 108, 104506.	1.1	9
179	Synthesis and characterization of ZnS tetrapods and ZnO/ZnS heterostructures. Thin Solid Films, 2012, 522, 40-44.	0.8	9
180	Structural transition behavior of ZnS nanotetrapods under high pressure. High Pressure Research, 2015, 35, 9-15.	0.4	9

#	Article	IF	CITATIONS
181	A new phase in TiB2-reinforced Ni–Al–Fe matrix composite. Journal of Materials Science, 1998, 33, 1183-1187.	1.7	8
182	Nanostructure Induced by Femtosecond Laser in Various OH-Contents Silicas. Journal of Nanoscience and Nanotechnology, 2008, 8, 1422-1426.	0.9	8
183	A high ON/OFF ratio organic film for photo- and electro-dual-mode recording. Applied Physics Letters, 2009, 94, 163309.	1.5	8
184	Well-aligned Nickel Nanochains Synthesized by a Template-free Route. Nanoscale Research Letters, 2010, 5, 597-602.	3.1	8
185	Enhanced photoluminescence from SiOx–Au nanostructures. CrystEngComm, 2013, 15, 10116.	1.3	8
186	Molecular Tilting Alignment on Ag@C Nanocubes Monitored by Temperature-Dependent Surface Enhanced Raman Scattering. Scientific Reports, 2017, 7, 12865.	1.6	8
187	Conductive electrodes of metallic-organic compound CH ₃ CuS nanowires for all-solid-state flexible supercapacitors. Nanoscale, 2021, 13, 6921-6926.	2.8	8
188	Giant Faraday rotation in diluted magnetic semiconductor Cd1â^'l‡Fel̈‡Tel̈‡. Solid State Communications, 1994, 92, 725-729.	0.9	7
189	Precipitations in an Yttrium-Containing Low-Expansion Superalloy. Journal of Materials Science, 1998, 33, 5069-5077.	1.7	7
190	Microanalytical study of the hexagonal phase in an yttrium-containing low expansion superalloy. Materials Science & Engineering A: Structural Materials: Properties, Microstructure and Processing, 1998, 241, 83-89.	2.6	7
191	Room temperature synthesis and one-dimensional self-assembly of interlaced Ni nanodiscs under magnetic field. Journal Physics D: Applied Physics, 2010, 43, 275002.	1.3	7
192	Effects of dopant content on optical and electrical properties of In2O3: W transparent conductive films. Rare Metals, 2012, 31, 168-171.	3.6	7
193	Structural stability and Raman scattering of CoPt and NiPt hollow nanospheres under high pressure. Progress in Natural Science: Materials International, 2013, 23, 382-387.	1.8	7
194	Efficient Synthesis of Bimetallic Pt ₃ Zn Alloy Nanocrystals with Different Shapes and their Enhanced Electrocatalytic Activity. ChemCatChem, 2019, 11, 6031-6038.	1.8	7
195	Au@Co ₂ P core/shell nanoparticles as a nano-electrocatalyst for enhancing the oxygen evolution reaction. RSC Advances, 2019, 9, 40811-40818.	1.7	7
196	Interface structure and strain controlled Pt nanocrystals grown at side facet of MoS2 with critical size. Nano Research, 2022, 15, 8493-8501.	5.8	7
197	HREM study of the NiAlFeî—,TiB2 composite fabricated by reaction compocasting. Materials Science & Engineering A: Structural Materials: Properties, Microstructure and Processing, 1999, 265, 95-99.	2.6	6
198	Microstructural and compositional characteristics of GaN films grown on a ZnO-buffered Si (111) wafer. Micron, 2004, 35, 475-480.	1.1	6

#	Article	IF	CITATIONS
199	Electron microscopy investigation of gallium oxide micro/nanowire structures synthesized via vapor phase growth. Micron, 2004, 35, 447-453.	1.1	6
200	Single-crystal star-like zinc oxide: synthesis, characterization and growth mechanism. Rare Metals, 2006, 25, 193-199.	3.6	6
201	Investigation of metal contacts to Nb-1.0wt.%-doped SrTiO3. Materials Science and Engineering B: Solid-State Materials for Advanced Technology, 2007, 138, 214-218.	1.7	6
202	Effect of cation addition on dielectric properties of TbMnO3. Physica B: Condensed Matter, 2007, 392, 147-150.	1.3	6
203	Delamination and magnetism softening of polycrystalline La0.9Ba0.1MnO3. Journal of Applied Physics, 2008, 103, 073907.	1.1	6
204	Pt-Based Nanostructures for Observing Genuine SERS Spectra of p-Aminothiophenol (PATP) Molecules. Applied Sciences (Switzerland), 2017, 7, 953.	1.3	6
205	Effective interbandgfactors in diluted magnetic semiconductor Cd1â^'xFexTe. Journal of Applied Physics, 1996, 80, 4421-4424.	1.1	5
206	Principle and Application of Tip-enhanced Raman Scattering. Plasmonics, 2018, 13, 1343-1358.	1.8	5
207	Microstructure and mechanical properties of NiAlCo–TiB2 composites. Materials Letters, 1999, 38, 54-57.	1.3	4
208	Two-step synthesis of Bi2Te3–Te nanoarrays with sheet–rod multiple heterostructure. Journal of Solid State Chemistry, 2010, 183, 2631-2635.	1.4	4
209	Spin-polarized Andreev reflection and spin accumulation in a quantum-dot Aharonov-Bohm interferometer with spin-orbit interaction effects. Journal of Applied Physics, 2011, 110, 033706.	1.1	4
210	An Investigation of Nickel Cobalt Oxide Nanorings Using Transmission Electron, Scanning Electron and Helium Ion Microscopy. Journal of Nanoscience and Nanotechnology, 2012, 12, 1094-1098.	0.9	4
211	Transmission Electron Microscopy. Springer Tracts in Modern Physics, 2018, , 69-203.	0.1	4
212	Surface Modifications of 2D-Ti3C2O2 by Nonmetal Doping for Obtaining High Hydrogen Evolution Reaction Activity: A Computational Approach. Catalysts, 2021, 11, 161.	1.6	4
213	Synthesization, characterization, and highly efficient electrocatalysis of chain-like Pt-Ni nanoparticles. Wuli Xuebao/Acta Physica Sinica, 2020, 69, 076101.	0.2	4
214	Dendritic porous silica nanoparticles with high-curvature structures for a dual-mode DNA sensor based on fluorometer and person glucose meter. Mikrochimica Acta, 2021, 188, 407.	2.5	4
215	Interface Interaction Dependent Growth of Carbon Nanostructures: An In Situ Study. Advanced Materials Interfaces, 2022, 9, .	1.9	4
216	Short-range order in nanoscale amorphous intergranular films in liquid-phase sintered silicon carbide. Applied Physics Letters, 2006, 89, 211902.	1.5	3

#	Article	IF	CITATIONS
217	Quenching-promoted anomalous electromagnetic behaviors of polycrystalline La0.67Ba0.33MnO3 compound by hydrogen annealing. Journal of Alloys and Compounds, 2007, 428, 40-43.	2.8	3
218	Template-Free Synthesis and Self-Assembly of Aligned Nickel Nanochains Under Magnetic Fields. Journal of Nanoscience and Nanotechnology, 2011, 11, 11128-11132.	0.9	3
219	Point defects in L10 FePt studied by molecular dynamics simulations based on an analytic bond-order potential. Science China: Physics, Mechanics and Astronomy, 2011, 54, 1429-1432.	2.0	3
220	Fabrication of Nano-Grating by Focused Ion Beam / Scanning Electron Microscopy Dual-Beam System. Key Engineering Materials, 0, 483, 66-69.	0.4	3
221	Focused ion beam built-up on scanning electron microscopy with increased milling precision. Science China: Physics, Mechanics and Astronomy, 2012, 55, 625-630.	2.0	3
222	Tailoring characteristic thermal stability of Ni-Au binary nanocrystals via structure and composition engineering: theoretical insights into structural evolution and atomic inter-diffusion. AIP Advances, 2014, 4, .	0.6	3
223	Bipolar Resistive Switching in Epitaxial Mn ₃ O ₄ Thin Films on Nb-Doped SrTiO ₃ Substrates. Chinese Physics Letters, 2016, 33, 067202.	1.3	3
224	Electric current-induced giant electroresistance in La _{0.36} Pr _{0.265} Ca _{0.375} MnO ₃ thin films. Chinese Physics B, 2017, 26, 047103.	0.7	3
225	One-dimensional hollow FePt nanochains: applications in hydrolysis of NaBH4 and structural stability under Ga+ ion irradiation. Nanotechnology, 2020, 31, 185704.	1.3	3
226	Interface modulation and physical properties of heterostructure of metal nanoparticles and two-dimensional materials. Wuli Xuebao/Acta Physica Sinica, 2022, 71, 066801.	0.2	3
227	Nonmetallic Active Sites on Nickel Phosphide in Oxygen Evolution Reaction. Nanomaterials, 2022, 12, 1130.	1.9	3
228	Superposed forward current–voltage characteristics in TbMnO3/n-Si and TbMnO3/p-Si heterostructures. Thin Solid Films, 2009, 517, 5872-5875.	0.8	2
229	The changes of capacitance–loss and current–voltage characteristics of LaMnO3+Î′/SrTiO3:Nb heterojunctions exposed to ambient air. Physics Letters, Section A: General, Atomic and Solid State Physics, 2010, 374, 625-627.	0.9	2
230	Scanning near-field acoustic microscope and its application. Science China Technological Sciences, 2011, 54, 126-130.	2.0	2
231	Growth and micromagnetic simulation of magnetite nanoparticles. Science China: Physics, Mechanics and Astronomy, 2011, 54, 1208-1212.	2.0	2
232	Quantum heat engine cycle working with a strongly correlated electron system. Science China: Physics, Mechanics and Astronomy, 2012, 55, 792-797.	2.0	2
233	Large enhancement of Blocking temperature by control of interfacial structures in Pt/NiFe/IrMn/MgO/Pt multilayers. AIP Advances, 2015, 5, 097146.	0.6	2
234	Structural, magnetic and transport properties of Pb2Cr1+xMo1â^'xO6 (â^'1â‰æâ‰≇/3). Journal of Solid State Chemistry, 2017, 246, 92-96.	1.4	2

#	Article	IF	CITATIONS
235	Resistive switching effects depending on Ni content in Au/NixPt(1â^'x) nanoparticle devices. RSC Advances, 2017, 7, 5445-5450.	1.7	2
236	Editorial for rare metals, special issue on nanomaterials and rechargeable battery applications. Rare Metals, 2017, 36, 305-306.	3.6	2
237	Correlation between pass-through flux of cobalt target and microstructure and magnetic properties of sputtered thin films. Rare Metals, 2021, 40, 975-980.	3.6	2
238	Synthesis and Self-Assembly of Ultrathin Ni _{<i>x</i>} Fe _{1â^'<i>x</i>} (OH) ₂ Nanodiscs via a Wet-Chemistry Method. Journal of Nanoscience and Nanotechnology, 2011, 11, 11028-11031.	0.9	1
239	Temperature independent leakage current in Au/TbMnO3/Y Ba2Cu3O7â^'x capacitors. Solid State Communications, 2012, 152, 123-126.	0.9	1
240	Theoretical investigation of geometries, stabilities, electronic and optical properties for advanced Agn@(ZnO)42 (n=6-18) hetero-nanostructure. AIP Advances, 2016, 6, 075023.	0.6	1
241	The Stability of High Metal-Loading Pt1/Fe2O3 Single-Atom Catalyst Under Different Gas Environment. Microscopy and Microanalysis, 2017, 23, 1898-1899.	0.2	1
242	First-principles investigation on Au _{<i>n</i>} @(ZnO) ₄₂ (n = 6–16) core-shell nanoparticles: structure stability and catalytic activity. Journal of Physics Condensed Matter, 2017, 29, 435701.	0.7	1
243	Constructing the Au–CoNi2S4 core–shell heterostructure to promote the catalytic performance for oxygen evolution. Journal Physics D: Applied Physics, 2021, 54, 425501.	1.3	1
244	Synthesis of Mn ₃ O ₄ Rings and Their Magnetic Properties. Science of Advanced Materials, 2010, 2, 428-431.	0.1	1
245	Nonâ€Local Electrostatic Gating Effect in Graphene Revealed by Infrared Nanoâ€Imaging. Small, 2021, , 2105687.	5.2	1
246	Influence of hydrogenation on the microstructure and crystallization of Zr-Cu-Ni-Al-Y metallic glass. Philosophical Magazine, 2003, 83, 2545-2556.	0.7	0
247	Large-Scale Synthesis of Uniform Nanotubes of a Nickel Complex by a Solution Chemical Route ChemInform, 2004, 35, no.	0.1	Ο
248	Synthesis and one-dimensional self-Assembly of aligned Ni nanochains under magnetic fields. , 2010, , .		0
249	Quantum phase transition in quarter-filled nanoclusters of manganite induced by element substitution at B site. Science China: Physics, Mechanics and Astronomy, 2011, 54, 1277-1282.	2.0	Ο
250	<i>A Special Section on</i> Magnetism at Nanoscale (IUMRS-ICA2010). Journal of Nanoscience and Nanotechnology, 2012, 12, 1004-1005.	0.9	0
251	Magnetization Reversal and Anisotropy with Chains of Superparamagnetic Ni Nanoparticles. Journal of Nanoscience and Nanotechnology, 2012, 12, 1036-1039.	0.9	0
252	Strong nonlinear currentâ \in "voltage behaviour in iron oxyborate. AlP Advances, 2014, 4, .	0.6	0

#	Article	IF	CITATIONS
253	Preface from guest editors. Progress in Natural Science: Materials International, 2016, 26, 211.	1.8	0
254	Electron/Ion Optics. Springer Tracts in Modern Physics, 2018, , 1-33.	0.1	0
255	The improvements of the dielectric performance of SmCrO3 by Zn doping. Physica B: Condensed Matter, 2021, 608, 412687.	1.3	0